

A reliable cw Lyman- α laser source for future cooling of antihydrogen

D. Kolbe · A. Beczkowiak · T. Diehl · A. Koglbauer · M. Sattler · M. Stappel · R. Steinborn · J. Walz

Received: date / Accepted: date

Abstract We demonstrate a reliable continuous-wave (cw) laser source at the $1S-2P$ transition in (anti)hydrogen at 121.56 nm (Lyman- α) based on four-wave sum-frequency mixing in mercury. A two-photon resonance in the four-wave mixing scheme is essential for a powerful cw Lyman- α source and is well investigated.

Keywords Lyman-alpha · Four-wave mixing · Antihydrogen

1 Introduction

Future high-resolution laser-spectroscopy of antihydrogen in a magnetic trap can provide very stringent tests of the fundamental symmetry between matter and antimatter (CPT symmetry) [1]. The two-photon $1S-2S$ transition is a good candidate for such precision experiments because of its natural linewidth of only 1.6 Hz at a transition frequency of 2 466 THz. The absolute frequency of this transition has already been measured in a beam with ordinary hydrogen to enormous precision [2,3]. However, the $1S-2S$ ($F = 1, m_F = 1 \rightarrow F = 1, m_F = 1$) transition frequency has a residual dependence on the magnetic field of 186 kHz per Tesla. This will broaden and shift the spectral line of antihydrogen atoms in a magnetic trap [4]. Reducing their spatial spread in the inhomogeneous magnetic field by cooling the antihydrogen atoms will thus be very important.

Laser cooling of ordinary hydrogen atoms in a magnetic trap to the milli-Kelvin temperature range has been demonstrated [5] with a pulsed laser source at the strong Lyman- α transition at 121.6 nm wavelength from the $1S$ ground state to the $2P$ excited state.

In addition to testing CPT there is also the intriguing prospect to measure the gravitational acceleration of antimatter for the first time using antihydrogen

D. Kolbe
Institut für Physik, Johannes Gutenberg-Universität Mainz and Helmholtz Institute Mainz,
D-55099 Mainz
Tel.: +49-6131-39-22385
Fax: +123-45-678910
E-mail: kolbed@uni-mainz.de

atoms [6]. The thermal motion of antihydrogen is a critical factor in this type of experiments and laser-cooling at Lyman-alpha to milli-Kelvin temperatures will be very beneficial. Ultimately, ultracold temperatures in the sub-milli-Kelvin range are desirable for practical experiments. These temperatures are beyond standard laser-cooling limits for (anti-)hydrogen. Novel cooling schemes for ultracold temperatures have been proposed [7, 8, 9, 10].

Producing coherent radiation at 121.6 nm (Lyman-alpha) is a challenge as there are no tunable lasers and nonlinear frequency-doubling crystals available for that spectral region. Sum-frequency generation of several incident laser beams utilizing the nonlinear susceptibility of atomic vapors and gases is commonly used to produce coherent radiation in the vacuum UV. Four-wave sum-frequency mixing produces the sum-frequency of three fundamental colors and has been employed to generate *pulsed* laser radiation at Lyman-alpha, typically using Krypton gas [11, 12, 13, 14].

Continuous coherent radiation at Lyman-alpha can have distinct advantages for laser-cooling of antihydrogen. For example, the cooling rate is not limited by the pulse to pause ratio and the smaller linewidth reduces pumping in untrapped states. An important difference, however, is that the power levels of continuous fundamental beams are many orders of magnitude lower than the peak powers typically used in pulsed Lyman-alpha generation. Continuous Lyman-alpha generation therefore uses resonances and near-resonances in the nonlinear optical medium.

In this paper a continuous coherent Lyman-alpha source is described which uses a four-wave mixing process in mercury with an exact two-photon resonance and a near one photon resonance of the fundamental beams. The paper is organized as follows: First the lasersystem for the fundamental beams and the Lyman-alpha production is explained. In the next part the influence of the two-photon resonance on the four-wave mixing process is discussed. In the third section we discuss the prospect of scaling the Lyman- α power.

2 Setup

The scheme of the four-wave mixing (FWM) process is shown in Figure 1 (a). A UV beam at 254 nm and a blue beam at 408 nm wavelength establish the two photon resonance between the 6^1S ground state and the 7^1S state of mercury. Additionally the UV beam can be tuned in a wide range around the 6^1S-6^3P intermediate one-photon resonance. The third beam determines the Lyman- α wavelength and is fixed at 545 nm.

The laser system producing the three fundamental beams is shown in the lower part of Figure 1(b). The beam at 254 nm is produced by a frequency-quadrupled Yb:YAG disc laser (ELS, VersaDisk 1030-50). Frequency-quadrupling is done with two resonant enhancement cavities, the first one using a lithium triborate crystal (LBO) as nonlinear medium, the second one using a β -barium borate crystal (BBO). From 2 W of infrared light at 1015 nm we get up to 200 mW of UV radiation. This system is in principle capable to produce up to 750 mW of UV light, for details see [15]. The second fundamental beam at 408 nm is produced by a frequency-doubled titanium:sapphire laser (Coherent, 899-21), pumped by a frequency doubled Nd:YVO₄ laser (Coherent, V10). The external frequency-doubling cavity uses a LBO crystal. From 1.5 W of IR light at 816 nm we get up to 500 mW of

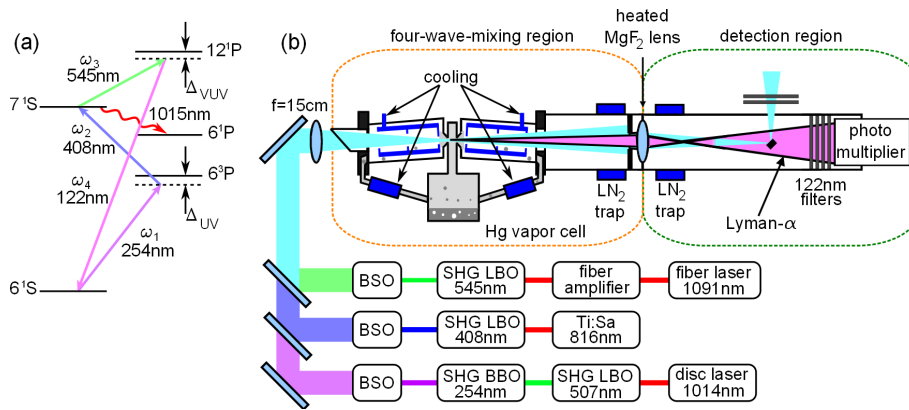


Fig. 1 Energy-level diagram of mercury, the FWM scheme and setup. (a), The UV laser (254 nm) is tuned close to the 6^1S-6^3P resonance, the blue laser (408 nm) establishes the two photon resonance with the 7^1S state. With the wavelength of the green laser (545 nm) the sum-frequency by four-wave mixing lies at the Lyman- α wavelength. Population in the 7^1S level decays mostly (80%) to the 6^1P state at a transition wavelength of 1014 nm. (b), Fundamental beams at 254 nm, 408 nm and 540 nm wavelength are produced by frequency-doubling or frequency-quadrupling strong cw infrared solid-state lasers. The beams are shaped, overlapped and focused into the mercury cell. In the FWM region Lyman- α generation takes place. Separating the Lyman- α from the fundamental beams is accomplished by the dispersion of a MgF_2 lens. Behind three Lyman- α filters a photomultiplier tube is used for detection. (SHG: second harmonic generation, LBO: lithium triborate crystal, BBO: β -barium borate crystal, BSO: beam shaping optics, LN_2 : liquid nitrogen)

blue light. The typical day to day power of this laser system is 300 mW. The third fundamental beam at 545 nm is produced with a 10 W fiber laser system at 1091 nm (Koheras, Adjustik and Boostik) and a modified commercial frequency-doubling cavity (Spectra Physics, Wavetrain). This system is capable of producing up to 4 W of green light [16]. However, at these high powers amplified back-reflections tend to damage the entrance facet of the amplification fiber. Getting the laser repaired by the manufacturer is tedious and very time-consuming. For the present experiments we therefore operate the fiber laser at 740 mW, a very conservative rating, which still gives 280 mW of green light.

The three fundamental beams are shaped by pairs of spherical and cylindrical lenses (see Figure 1(b)). The beams are overlapped at dichroic mirrors and focused into the mercury cell using a fused silica lens with a focal length of 15 cm. The mercury cell can be heated up to 240°C providing a mercury vapor density of up to $N = 1.1 \times 10^{24}\text{m}^{-3}$. Outside the focus region cooled baffles and helium buffer gas with a pressure of 100 mbar are used to avoid condensation of mercury on the optics. The four-wave mixing region is separated from the detection region by a vacuum sealed MgF_2 lens which performs separation of the Lyman- α light from the fundamental beams (see Figure 1(b)). Due to the dispersion of this lens the focal length differs for the Lyman- α wavelength ($f = 21.5\text{ cm}$ at 540 nm, $f = 13\text{ cm}$ at 122 nm). A tiny mirror is placed in the focus of the fundamental beams to reflect them to the side. The Lyman- α beam is large at the fundamental focus and therefore the mirror just casts a shadow in the Lyman- α beam, causing $\approx 30\%$ loss. A solar-blind photomultiplier tube is used for detection of the Lyman- α photons. Background is suppressed by three 122 nm filters. The overall detection

efficiency due to losses in the MgF₂ lens, the tiny mirror, the three filters and the photomultiplier efficiency is 6×10^{-5} . IR light from the 7^1S-6^1P decay at 1014 nm (see also Figure 1(a)) can be detected as a measure of the beam overlap of the blue and the UV beam.

3 Two-photon resonance

To enhance the third order nonlinear susceptibility exploitation of a two-photon resonance has been investigated [17]. For a powerful cw Lyman- α source the utilisation of a two-photon resonance is essential [18, 19, 20]. We use the 6^1S-7^1S two-photon resonance with a transition wavelength of 156.5 nm. The nonlinear susceptibility $\chi^{(3)}$ responsible for the FWM in the case of a close two-photon resonance can be expressed as [21]:

$$\chi^{(3)} = \frac{N}{6\epsilon_0\hbar^3} S(\omega_1, \omega_2) \chi_{12} \chi_{34} \quad (1)$$

with the two partial susceptibilities

$$\chi_{12} = \sum_m \left(\frac{p_{nm}p_{mg}}{\omega_{gm} - \omega_1} + \frac{p_{nm}p_{mg}}{\omega_{gm} - \omega_2} \right) \quad , \quad (2)$$

$$\chi_{34} = \sum_\nu \left(\frac{p_{n\nu}p_{\nu g}}{\omega_{g\nu} - \omega_4} + \frac{p_{n\nu}p_{\nu g}}{\omega_{g\nu} + \omega_3} \right) \quad , \quad (3)$$

and the term describing the two-photon resonance

$$S(\omega_1 + \omega_2) = \frac{1}{\omega_{ng} - (\omega_1 + \omega_2)} \quad . \quad (4)$$

Identical linear polarization of the fundamental beams is assumed. Summing over m and ν in the partial susceptibilities includes all excited states that connect to the 6^1S ground state (index n) and the 7^1S state (index g) by dipole transitions. The dipole matrix elements p_{ab} can be obtained from the oscillator strengths f_{ab} tabulated in [22]. The function $S(\omega_1 + \omega_2)$ contains the enhancement due to the two-photon resonance. The homogeneous line-broadening Γ_{7S}^{hom} consisting of natural line width and pressure-broadening is included by adding the term $-i\Gamma_{7S}^{hom}/2$ in the denominator of equation (4). The Doppler-broadening is included by adding the Doppler-shift kv of an atom with velocity v and integrating over the one dimensional Boltzmann velocity distribution. The two-photon resonance has two effects: On the one hand, the two-photon resonance enhances the FWM process according Equation 1. On the other hand, it transfers population to the 7^1S two-photon state which can be detected with the fluorescence light of the 7^1S-6^1P transition at 1015 nm (see Figure 1(a)). In the next two subsections we will first discuss the effect of polarization of the fundamental beams on the FWM process and the population transfer and second introduce a laser process on the 7^1S-6^1P transition as a adjustment tool.

3.1 Polarization dependence

In Equation 1 we assumed equal polarization of all fundamental beams. In general the third order nonlinear susceptibility is a tensor of the order of 4 including all possible polarization states of the fundamental beams. In the case of two-photon resonant four-wave mixing the efficiency depends critically on the polarisation of the UV and blue beams which establish the two-photon resonance [23]. In Figure 2 the normalized IR signal of the decay of the 7^1S and the normalized Lyman- α signal out of the four-wave mixing process versus the angle between the linear polarization of the UV beam to the blue beam is shown. It can be clearly seen that both signals are equally modulated by the polarisation. In the case of the two-photon signal excitation to the 7^1S state can only occur with equal polarization of the fundamental light fields. The excitation is therefore modulated by the intensity of the UV beam projected on the polarisation vector of the blue beam resulting in a modulation proportional to a cosine function. The same behavior is observed in the Lyman- α signal showing that the two-photon resonance in the nonlinear susceptibility depends of the polarisation in the same manner. The phase of the cosine function in Figure 2 is extracted from the Lyman- α signal. The polarisation of the green beam in contrast did not have any influence on the four-wave mixing efficiency as was checked by rotating the green polarization and has already been well investigated [23].

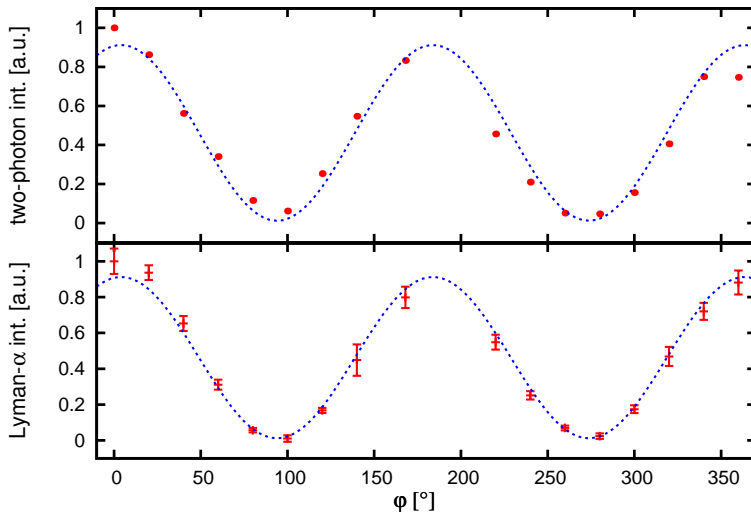


Fig. 2 Polarisation dependence of the IR and Lyman- α signal. Normalized IR (top) and Lyman- α (bottom) intensity versus the angle φ between the polarization of the blue and UV beam. Both signals are modulated in the same way following a cosine function. Period and phase of the function is fitted to the Lyman- α signal.

3.2 Two-photon laser induced stimulated emission

Due to the short lifetime of the 6^1P state (1.5 ns) compared to the two-photon 7^1S state (32 ns) a high enough two-photon excitation rate can establish a laser process on the 7^1S-6^1S transition at 1015 nm (see Figure 1(a)). This two-photon laser induced stimulated emission (TALISE) has been well investigated [24,25]. It does not influence the four-wave mixing process in this low loss (due to conversion) regime. Due to the strong increase in the IR power at the threshold condition of the TALISE process the IR signal is a perfect diagnostic tool for the overlap of the blue and UV beam. In Figure 3 the IR signal and Lyman- α versus the detuning to the two photon resonance is shown. At the bottom the Lyman- α signal peaks at the two-photon resonance condition of every mercury isotope resulting in four peaks. The threshold condition for TALISE depends of the density of the mercury atoms and therefore differs for the various isotopes. At the right of Figure 3 the threshold condition of the 202 and 200 isotopes (the most abundant isotopes in a natural mercury mixture [26]) are fulfilled resulting in two peaks in the IR signal (top). The IR signal is at threshold much more critical on the alignment of the overlap of the blue and the UV beam. Better alignment (left) boosts the IR signal to a greater extent than the Lyman- α signal which provides a much more sensitive adjustment.

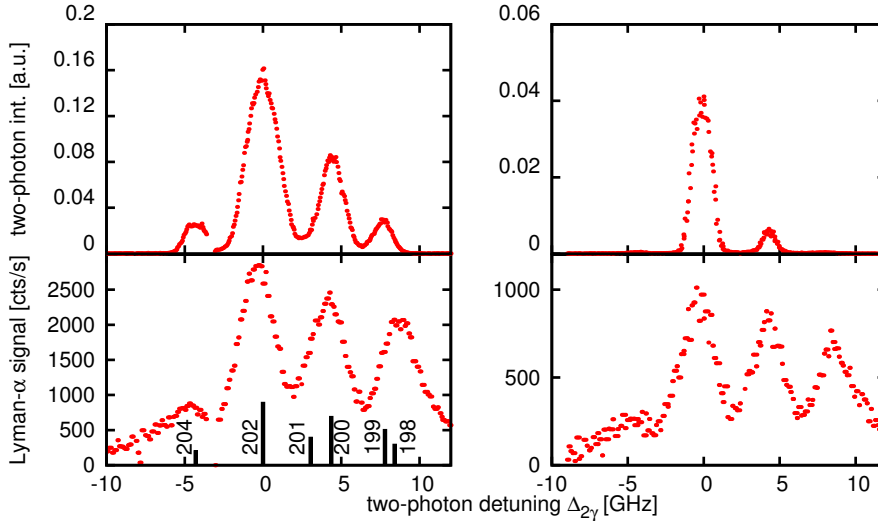


Fig. 3 Alignment dependence of the IR and Lyman- α signal. IR (top) and Lyman- α (bottom) power at scans across the two-photon resonance. Two-photon detuning $\Delta_{2\gamma} = \omega_{6^1S-7^1S} - (\omega_1 + \omega_2)$ determines the detuning to the two-photon resonance of the 202 mercury isotope. At threshold of the TALISE process the IR power is much more critical on the alignment of the beams than the Lyman- α power. Power increase from bad alignment (right) to good alignment (left) differs for the IR and Lyman- α signal. Vertical bars indicate the positions and abundances of the different isotopes. Note the different scales.

4 Lyman- α power scalability

In the case of four-wave mixing with no loss of the fundamental beams due to absorption and conversion the power at Lyman- α is proportional to the power-product of the fundamental beams [27]:

$$P_4 \propto P_1 P_2 P_3 \quad , \quad (5)$$

where P_4 is the power at Lyman- α and $P_{1,2,3}$ is the power of the UV, blue and green fundamental beam respectively. The Lyman- α power was measured to be perfectly linear to the green power. We achieved a maximum power of 0.3 nW at fundamental powers of $P_1 = 130$ mW, $P_2 = 324$ mW and $P_3 = 185$ mW. The power levels required for Doppler-cooling of antihydrogen in a magnetic trap are rather low: With 1 nW of Lyman- α we expect cooling times in the order of minutes [19]. Nevertheless, due to losses at the beam transfer from the four-wave mixing region to the antihydrogen trap center and for reducing of cooling time a high power Lyman- α source is desired. With full fundamental laser powers we expect Lyman- α powers up to 65 nW. Further increase could be performed by enhancing the fundamental powers in separated cavities with a shared focused cavity arm where all beams are overlapped and FWM takes place. With typical coupling efficiencies of $\approx 70\%$ and estimated enhances of a factor of 50 for every fundamental beam an increase in Lyman- α power of a factor of 40 000 seems feasible.

5 Conclusion

A cw Lyman- α laser source is a key tool for future experiments on antihydrogen. We presented a reliable Lyman- α source with powers up to 0.3 nW for an estimated cooling time of antihydrogen in the region of minutes. The 6^1S-7^1S two-photon resonance in mercury is crucial for the four-wave mixing efficiency.

Acknowledgements We acknowledge support from the Bundesministerium für Bildung und Forschung.

References

1. R. Bluhm, V.A. Kostelecky, N. Russell, Physical Review Letters **82**(11), 2254 (1999)
2. M. Niering, R. Holzwarth, J. Reichert, P. Pokasov, T. Udem, M. Weitz, T.W. Hänsch, P. Lemonde, G. Santarelli, M. Abgrall, P. Laurent, C. Salomon, A. Clairon, Physical Review Letters **84**(24), 5496 (2000)
3. M. Fischer, N. Kolachevsky, M. Zimmermann, R. Holzwarth, T. Udem, T.W. Hänsch, M. Abgrall, J. Grünert, I. Maksimovic, S. Bize, H. Marion, F.P.D. Santos, P. Lemonde, G. Santarelli, P. Laurent, A. Clairon, C. Salomon, M. Haas, U.D. Jentschura, C.H. Keitel, Phys. Rev. Lett. **92**(23), 230802 (2004)
4. C.L. Cesar, Physical Review A **64**(2), 023418 (2001)
5. I.D. Setija, H.G.C. Werij, O.J. Luiten, M.W. Reynolds, T.W. Hijmans, J.T.M. Walraven, Physical Review Letters **70**(15), 2257 (1993)
6. G. Gabrielse, Hyperfine Interactions **44**(1-4), 349 (1988)
7. J. Walz, T.W. Hänsch, General Relativity and Gravitation **36**(3), 561 (04)
8. P. Pérez, L. Liskay, J.M. Rey, O. Delferrière, V. Blideanu, M. Carty, A. Curtoni, N. Ruiz, Y. Sauce, Applied Surface Science **255**(1), 33 (2008)

-
9. U. Warring, M. Amoretti, C. Canali, A. Fischer, R. Heyne, J.O. Meier, C. Morhard, A. Kellerbauer, Phys. Rev. Lett. **102**(4), 043001 (2009)
 10. A. Fischer, C. Canali, U. Warring, A. Kellerbauer, S. Fritzsche, Phys. Rev. Lett. **104**(7), 073004 (2010)
 11. R. Mahon, T.J.M. Ilrath, D.W. Koopman, Applied Physics Letters **33**(4), 305 (1978)
 12. D. Cotter, Optics Communications **31**(3), 397 (1979)
 13. R. Wallenstein, Optics Communications **33**(1), 119 (1980)
 14. J.P. Marangos, N. Shen, H. Ma, M.H.R. Hutchinson, J.P. Connerade, Journal of the Optical Society of America B **7**(7), 1254 (1990)
 15. M. Scheid, F. Markert, J. Walz, J. Wang, M. Kirchner, T.W. Hänsch, Optics Letters **32**(8), 955 (2007)
 16. F. Markert, M. Scheid, D. Kolbe, J. Walz, Optics Express **15**(22), 14476 (2007)
 17. A.V. Smith, W.J. Alford, G.R. Hadley, J. Opt. Soc. Am. B **5**(7) (1988)
 18. K.S.E. Eikema, J. Walz, T.W. Hänsch, Phys. Rev. Lett. **83**(19), 3828 (1999)
 19. J. Walz, A. Pahl, K.S.E. Eikema, T.W. Hänsch, Nuclear Physics A **692**(1-2), 163 (2001)
 20. M. Scheid, D. Kolbe, F. Markert, T.W. Hänsch, J. Walz, Optics Express **17**(14), 11274 (2009)
 21. A.V. Smith, W.J. Alford, J. Opt. Soc. Am. B **4**(11) (1987)
 22. W.J. Alford, A.V. Smith, Physical Review A **36**(2) (1987)
 23. R. Irrgang, M. Drescher, F. Gierschner, M. Spieweck, U. Heinzmann, Measurement Science and Technology **9**(3), 422 (1998)
 24. J. Amorim, G. Baravian, Optics Communications **192**(3-6), 277 (2001)
 25. D. Kolbe, M. Scheid, A. Koglbauer, J. Walz, Opt. Lett. **35**(16), 2690 (2010)
 26. M.G. Zadnik, S. Specht, F. Begemann, International Journal of Mass Spectrometry and Ion Processes **89**(1), 103 (1989)
 27. G.C. Bjorklund, IEEE Journal of Quantum Electronics **11**(6), 287 (1975)